

Arteriosclerosis, Thrombosis, and Vascular Biology



JOURNAL OF THE AMERICAN HEART ASSOCIATION

Application of Infrared Laser to the Zebrafish Vascular System : Gene Induction, Tracing, and Ablation of Single Endothelial Cells

Eiji Kimura, Tomonori Deguchi, Yasuhiro Kamei, Wataru Shoji, Shunsuke Yuba and Jiro Hitomi

Arterioscler Thromb Vasc Biol. 2013;33:1264-1270; originally published online March 28, 2013;

doi: 10.1161/ATVBAHA.112.300602

Arteriosclerosis, Thrombosis, and Vascular Biology is published by the American Heart Association, 7272 Greenville Avenue, Dallas, TX 75231

Copyright © 2013 American Heart Association, Inc. All rights reserved.

Print ISSN: 1079-5642. Online ISSN: 1524-4636

The online version of this article, along with updated information and services, is located on the World Wide Web at:

<http://atvb.ahajournals.org/content/33/6/1264>

Data Supplement (unedited) at:

<http://atvb.ahajournals.org/content/suppl/2013/03/28/ATVBAHA.112.300602.DC1.html>

Permissions: Requests for permissions to reproduce figures, tables, or portions of articles originally published in *Arteriosclerosis, Thrombosis, and Vascular Biology* can be obtained via RightsLink, a service of the Copyright Clearance Center, not the Editorial Office. Once the online version of the published article for which permission is being requested is located, click Request Permissions in the middle column of the Web page under Services. Further information about this process is available in the [Permissions and Rights Question and Answer](#) document.

Reprints: Information about reprints can be found online at:

<http://www.lww.com/reprints>

Subscriptions: Information about subscribing to *Arteriosclerosis, Thrombosis, and Vascular Biology* is online at:

<http://atvb.ahajournals.org/subscriptions/>

Application of Infrared Laser to the Zebrafish Vascular System

Gene Induction, Tracing, and Ablation of Single Endothelial Cells

Eiji Kimura, Tomonori Deguchi, Yasuhiro Kamei, Wataru Shoji, Shunsuke Yuba, Jiro Hitomi

Objective—Infrared laser–evoked gene operator is a new microscopic method optimized to heat cells in living organisms without causing photochemical damage. By combining the promoter system for the heat shock response, infrared laser–evoked gene operator enables laser-mediated gene induction in targeted cells. We applied this method to the vascular system in zebrafish embryos and demonstrated its usability to investigate mechanisms of vascular morphogenesis in vivo.

Approach and Results—We used double-transgenic zebrafish with *fli1:nEGFP* to identify the endothelial cells, and with *hsp:mCherry* to carry out single-cell labeling. Optimizing the irradiation conditions, we finally succeeded in inducing the expression of the mCherry gene in single targeted endothelial cells, at a maximum efficiency rate of 60%. In addition, we indicated that this system could be used for laser ablation under certain conditions. To evaluate infrared laser–evoked gene operator, we applied this system to the endothelial cells of the first intersegmental arteries, and captured images of the connection between the vascular systems of the brain and spinal cord.

Conclusions—Our results suggest that the infrared laser–evoked gene operator system will contribute to the elucidation of the mechanisms underlying vascular morphogenesis by controlling spatiotemporal gene activation in single endothelial cells, by labeling or deleting individual vessels in living embryos. (*Arterioscler Thromb Vasc Biol.* 2013;33:1264-1270.)

Key Words: endothelial cells ■ gene expression ■ heat-shock response ■ infrared rays
■ morphogenesis ■ zebrafish

The vascular system is necessary for blood supply, thereby providing oxygen and nutrition to all organs. Using time-lapse analysis of living zebrafish embryos transgenic for *fli1:EGFP*, in which the endothelial cells specifically expressed enhanced green fluorescent protein, we studied the formation of the vascular system of the brain during early ontogeny. Our morphological data have indicated that vascular morphogenesis proceeded with a regular time course to form a uniform structure, which led to the subsequent interest in understanding the underlying mechanisms. Although many studies have investigated the morphogenesis of a developing embryo, little is known about the mechanisms underlying the formation of the vascular system. At present, vasculogenesis and angiogenesis have been advocated as being part of vascular development. In vasculogenesis, the primary vascular network was first formed from the lateral plate mesoderm, and then, further blood vessels were generated by both sprouting and nonsprouting angiogenesis. The vascular plexus was rapidly remodeled, and flow dynamics were believed to play critical roles in determining the processes underlying vascular morphogenesis, including the differentiation of arteries and veins.¹ However, the formation of the early vascular network in the

developing trunk progressed without blood flow in zebrafish²; similar data have been obtained for the vascular development of the brain (unpublished data). These results suggest that vascular morphogenesis is regulated by genetic cues, indicating that precise analysis of gene function is required for its complete understanding.

Several methods have been used to analyze specific gene functions associated with morphogenesis in developing embryos. Recently, the use of conventional knockout mice using the Cre-loxP system³ or microelectroporated chicken embryos⁴ has become common technique. To a certain extent, spatiotemporal gene regulation can be achieved by these methods, whereas strict gene regulation in a single cell is obligatory for the precise understanding of its function, especially in a noncell autonomous system, such as morphogenesis. In contrast, the heat shock protein (*hsp*) promoter has frequently been used for ectopic gene induction in vivo. A combination of the *hsp* promoter and laser irradiation enables the spatiotemporal regulation of gene induction in targeted cells.^{5,6} The heat shock response is widely conserved in all organisms,⁷ and is thus easily applied to both model and nonmodel organisms in the absence of specific DNA enhancers. The guidance mechanism

Received on: October 5, 2012; final version accepted on: March 10, 2013.

From the Department of Anatomy, Iwate Medical University, Iwate, Japan (E.K., J.H.); Tissue Engineering Research Group, Health Research Institute, National Institute of Advanced Industrial Science and Technology, Hyogo, Japan (T.D., S.Y.); Spectrography and Bioimaging Facility, National Institute for Basic Biology Core Research Facilities, National Institute for Basic Biology, Aichi, Japan (Y.K.); and Department of Project Programs, Institute of Development, Aging and Cancer, Tohoku University, Miyagi, Japan (W.S.).

The online-only Data Supplement is available with this article at <http://atvb.ahajournals.org/lookup/suppl/doi:10.1161/ATVBAHA.112.300602/-/DC1>.

Correspondence to Eiji Kimura, Department of Anatomy, Iwate Medical University, Iwate 020-3694, Japan. E-mail eijik@iwate-med.ac.jp

© 2013 American Heart Association, Inc.

Arterioscler Thromb Vasc Biol is available at <http://atvb.ahajournals.org>

DOI: 10.1161/ATVBAHA.112.300602

of spinal motor axons by *semaphorin 3a1* has been reported using sublethal laser-induced transgene expression in targeted single neurons.⁸

Because this method used a coumarin dye laser (440 nm), it may be suitable to irradiate superficial tissue, but not deep-lying tissue, such as the vasculature. In addition, the mechanism underlying the activation of the *hsp* promoter is still unclear, although the DNA damage induced by laser irradiation might be involved. We thus focused on infrared (IR) laser (1480 nm), which has a superior ability to heat water and can efficiently access deep-lying tissues. The IR laser-evoked gene operator (IR-LEGO) system is a new microscopic method optimized to heat cells by using an IR laser. We confirmed that this system was efficient in regulating spatiotemporal gene expression, and reported IR laser-mediated gene induction in single targeted cells in nematodes (*Caenorhabditis elegans*),⁹ and the local gene expression in various tissues, such as the muscle, notochord, and retina in some living vertebrates, for example, zebrafish (*Danio rerio*) and medaka (*Oryzias latipes*).¹⁰

In this study, we applied this IR-LEGO system to the vascular system in zebrafish and established, to the best of our knowledge, for the first time, an excellent method to induce laser-mediated gene expression in single targeted endothelial cells in vivo. We optimized the irradiation conditions, which resulted in raising the efficiency of laser-mediated gene induction up to 60%. Furthermore, we applied this method to the endothelial cells of the first intersegmental arteries (SeAs) to evaluate the system, and revealed their contribution in connecting the vascular systems of the brain and spinal cord. Our data indicate that the IR-LEGO system is a useful method for the investigation of vascular morphogenesis in vivo.

Materials and Methods

Materials and Methods are available in the online-only Supplement.

Results

IR Laser-Mediated Gene Expression in Targeted Single Endothelial Cells

Previously, we reported IR laser-mediated local gene induction in various tissues in some vertebrates and higher plants.¹⁰ In this study, we attempted to control gene expression in the single endothelial cells in zebrafish. We identified each single endothelial cell by using zebrafish transgenic for *fti1:nEGFP*, and we used the IR laser to irradiate them individually, and induced the expression of mCherry by using the IR-LEGO (Figure 1A–1C). The efficiency of IR laser in targeting the cell was confirmed by observing the reduction of fluorescence intensity (Figure 1D–1F). To optimize the irradiation conditions, we applied various irradiation powers (17.4, 15.6, 13.8, 12.1, and 10.8 mW) to each single SeA endothelial cell for 1 s, respectively. After 18 hours, we evaluated laser-mediated gene induction by using confocal microscopy (Figure 2). Two types of cells expressed mCherry fluorescence after irradiation with various IR laser-power sources: one type included the nontargeted muscle cells that were superficial to the irradiated endothelial cells (Figure 2, arrows), and the other type included the targeted single endothelial cells (Figure 2,

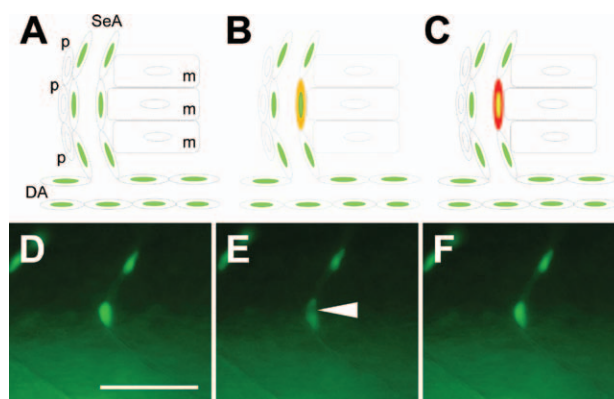


Figure 1. IR laser irradiation procedure for targeting single endothelial cells. **A–C**, Schematic illustration of laser-mediated gene induction in the targeted endothelial cell. IR laser irradiation was carried out under observation with a fluorescent microscope to distinguish the to-be-targeted single endothelial cells labeled with enhanced green fluorescent protein (EGFP) in each nucleus (**A**). They were individually heated, and then, the heat shock protein promoter was activated (**B**). A few hours later, the cytoplasmic expression of mCherry was induced. The irradiated nucleus was finally colored yellow because of superimposition with the nucleus-localized EGFP in a merged fluorescent image (**C**). Pericytes (p) and muscle cells (m) surrounding the vessels could not be observed by fluorescence microscopy. **D–F**, Verification of IR-irradiation could be confirmed by fluorescence. Before (**D**), during (**E**), and after irradiation (**F**). Reduction of the fluorescent intensity of nucleus-localized EGFP was observed only in the heating area during irradiation (**E**, arrowhead). Scale bar, 50 μ m. DA indicates dorsal aorta; and SeA, intersegmental artery.

arrowheads). To investigate the optimal irradiation conditions, we compared IR laser power-dependent gene induction more precisely; 20 single endothelial cells were irradiated with each laser power condition. The efficiency of gene induction in the targeted and nontargeted cells is summarized in Table 1. The 1-s-long irradiation with IR laser at 17.4, 15.6, 12.8, 12.1, and 10.8 mW could induce gene expression in the targeted single endothelial cells; IR laser irradiation at 12.1 mW achieved the highest efficiency of 30% (6/20). In contrast, gene expression in the nontargeted cells, such as muscle cells, was also confirmed in each irradiated embryo. Suppressing gene induction in the nontargeted cells was difficult under conditions of higher power, such as 17.4 and 15.6 mW (Figure 2A and 2B, and Table 1). However, reducing the irradiation power decreased the efficiency in nontargeted cells (Table 1), and led to the weakening of the fluorescent intensity (Figure 2C–2E). In this case, the 1-s-long irradiation with the 10.8-mW IR laser had the least influence on the nontargeted cells, but the efficiency to induce the expression of mCherry in the targeted cells was inadequate. We, therefore, determined that the 1-s-long irradiation with the 12.1-mW IR laser was the optimal condition to induce gene expression in the endothelial cells, with a lesser influence on the nontargeted cells (Figure 2D and Table 1). Furthermore, we studied the time course of laser-mediated gene expression. We applied various irradiation powers (17.4, 15.6, 13.8, 12.1, and 10.8 mW) to single SeA endothelial cells in the same embryo for 1 s each; mCherry expression was then observed by fluorescence microscopy every 2 hours after irradiation (Figure IIA–IID in the online-only Data Supplement), and 18 hours after

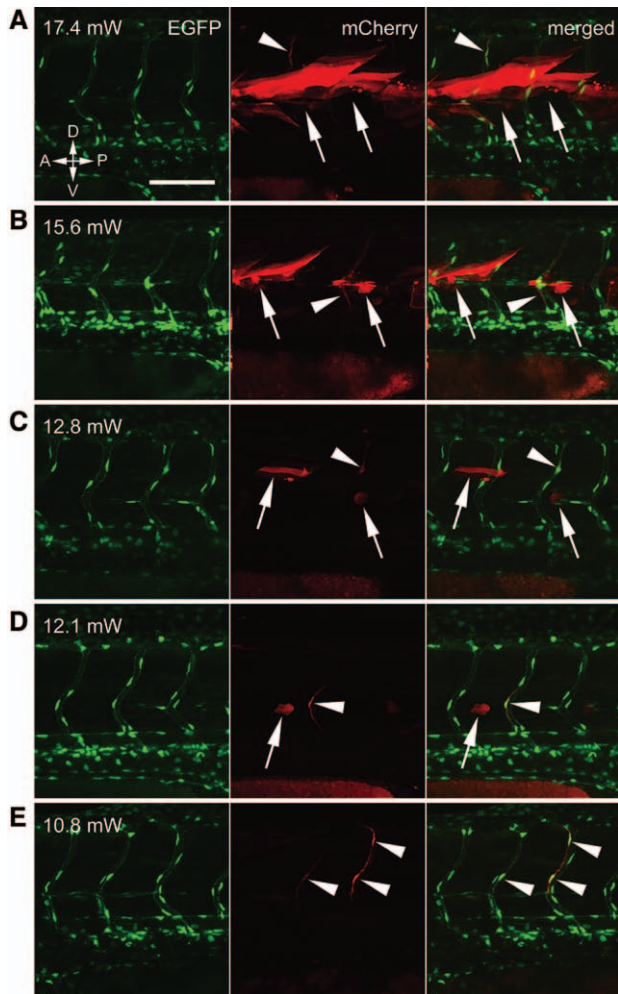


Figure 2. IR laser power-dependent mCherry expression in targeted and nontargeted cells. We applied irradiation with an IR laser at 17.4 mW (A), 15.6 mW (B), 12.8 mW (C), 12.1 mW (D), and 10.8 mW (E) for 1 s to the targeted single endothelial cells, and observed them with confocal microscope 18 hours later. Gene induction of mCherry in the targeted endothelial cells (arrowheads) and nontargeted cells (arrows). The direction of the embryo is indicated. Scale bar, 100 μ m. A indicates anterior; D, dorsal; P, posterior; and V, ventral.

irradiation by confocal microscopy (Figure IIE–IIG in the online-only Data Supplement). The first 2 irradiations at 17.4 and 15.6 mW resulted in mCherry induction only in the nontargeted muscle cells (Figure IIF and IIG in the online-only Data Supplement, arrows), whereas the fourth irradiation at 12.1 mW succeeded in inducing laser-mediated gene expression in the targeted single endothelial cell (Figure IIF and IIG in the online-only Data Supplement, arrowheads). The expression of mCherry in the nontargeted muscle cells was mild at 4 hours after the irradiation (Figure IIB in the online-only Data Supplement, arrows), but grew stronger with time (Figure IIC and IID in the online-only Data Supplement, arrows). The targeted endothelial cell also expressed mCherry 6 hours after irradiation, which also grew stronger (Figure IIC and IID in the online-only Data Supplement, arrowheads). These observations will be valuable to assess the effect of the expression of particular genes in endothelial cells by using this system.

Table 1. Efficiency of Laser-Mediated Gene Induction at Various Infrared Laser Powers

Condition of Irradiation (1-s-Long Single Pulse), mW	Gene Induction in Targeted Endothelial Cells	Gene Induction in Nontargeted Cells
17.4	2/20 (10%)	20/20 (100%)
15.6	3/20 (15%)	18/20 (90%)
12.8	2/20 (10%)	10/20 (50%)
12.1	6/20 (30%)	4/20 (20%)
10.8	3/20 (15%)	2/20 (10%)

The number of mCherry-induced endothelial cells and mCherry-induced nontargeted cells, and the percentage of each count are indicated.

Efficiency of IR Laser-Mediated Gene Induction

As we succeeded in optimizing the irradiation conditions to induce laser-mediated gene expression in single targeted endothelial cells with minimum effect on nontargeted cells, we next investigated its efficiency by using this optimized condition (12 mW for 1 s). We selected 1 endothelial cell from each SeA, and in total, 70 single endothelial cells from the SeAs at 2 dpf were irradiated. As a result, the gene expression of mCherry was induced in 25 irradiated single endothelial cells with an efficiency of 35.7% (25/70). The expression in nontargeted cells was also observed, and its efficiency was 12.9% (9/70). We then decreased the irradiation power from 12 mW to 10.8 mW and increased the frequency from 1 time to 3 times (pulsed irradiation) to further improve efficiency. Under these conditions, we used the IR laser to completely irradiate 30 single endothelial cells. As a result, the gene expression of mCherry was induced in 18 irradiated endothelial cells, that is, the efficiency increased to 60% (18/30). Accordingly, the gene expression in nontargeted cells also increased to 33.3% (10/30). These results are summarized in Table 2, and select images of irradiated embryos in 2 different conditions have been presented as examples (Figures III and IV in the online-only Data Supplement). Comparison of these results suggests an inconvenient relationship, whereby increasing the frequency of irradiation significantly improves the efficiency of laser-mediated gene induction in the targeted cells, whereas the induction in nontargeted cells increased at the same time. However, the maximum induction rate of 60% was an adequate achievement with respect to controlling spatiotemporal gene expression in vivo. Our data suggest that the IR-LEGO system will be a powerful tool for the functional analysis of a particular gene in vivo associated with vascular morphogenesis, especially for a system that satisfies the requirement of complete deletion of gene induction in nontargeted cells.

Tracing the Targeted Single Endothelial Cells of the First Intersegmental Arteries

The induction of mCherry in the targeted endothelial cells enabled us to trace them throughout the ontogeny within the period of mCherry expression. We used this advantage to analyze the formation of the connecting portion of the vascular systems between the brain and spinal cord. Morphogenesis in this region has previously been reported using microangiography, and it showed that the primordial hindbrain channel (PHBC) and basilar artery (BA) extended caudally and connected with

Table 2. Efficiency of Laser-Mediated Gene Induction Under Optimized Conditions

Condition of Irradiation	Gene Induction in Targeted Endothelial Cells	Gene Induction in Nontargeted Cells
1-s-long single pulse of 12 mW laser	25/70 (35.7%)	9/70 (12.9%)
1-s-long 3 pulses of 10.8 mW laser (total, 3 s)	18/30 (60%)	10/30 (33.3%)

The number of mCherry-induced endothelial cells and mCherry-induced nontargeted cells, and the percentage of each count are indicated.

the dorsal longitudinal anastomotic vessel (DLAV) at 1.5 to 2.0 dpf, which was formed by the longitudinal anastomosis of the branches of the intersegmental vessels in the dorsal region of the neural tube (schematic illustrations are indicated in Figure 3A and 3B).¹¹ However, this method allowed the observation of only the lumen of the vessels, not the growing vessels before tube formation, and therefore, it is still unknown how these vessels were connected. We focused on the first SeAs as the candidate connecting these vascular systems, because their contribution to this connection had not been revealed. They could be observed obviously in the *flil:nEGFP* transgenic zebrafish embryos (Figure 3C), although they could not be identified by microangiography (Figure 3A). To investigate their role in this connection, we labeled and traced them after irradiation with the IR laser. After 16 to 18 hours, we confirmed the localization of the green/red fluorescence-labeled endothelial cells dorsally and laterally after these vessels became connected (Figure 3D and 3E). We applied 2 irradiating conditions for these labeling experiments; a 1-s-long single pulse from a 12-mW laser and three 1-s-long pulses with a 10.8-mW laser (pulse irradiation). The efficiency labeling of the first SeA of the former condition was 16.7% (3/18), and that of the latter was 20% (2/10). In total, we succeeded in labeling 5 targeted endothelial cells of the first SeAs, and the mCherry-labeled cells from the first SeAs were located in the connecting portion of the BA, PHBC, and DLAV, suggesting that the endothelial cells of first SeAs bridge the vascular systems of the brain and spinal cord. Our labeling data for the first SeAs are summarized in Figure 3F and 3G, and we assume that the first SeAs could not be represented by microangiography because of the lack of connection with the dorsal aorta.

Ablation of the Endothelial Cells in the First Segmental Arteries

Because IR-laser is capable of heating water, irradiation overdose can cause injury to the cells. We used this property to ablate particular vessels in the formation of the vascular system. For the first target of the ablation study, we again selected the first SeA. We applied a high-power flash irradiation of IR laser (70 mW for 8-ms) to the endothelial cells, and evaluated its influence over the morphogenesis of the vascular systems between the brain and spinal cord. Whether this attempt to ablate the targets succeeded was judged by the disappearance of nucleus-localized enhanced green fluorescent protein. The change in the connecting portion of the BA, PHBC, and DLAV was observed by confocal microscopy 16 to 18 hours

after ablation, in both lateral and dorsal views (Figure 4A and 4B). Although PHBC usually extends obliquely from the caudal head region to the dorsal end of the second SeA, PHBC on the irradiated side did not connect to the second SeA; that is, their extension stopped around the ablated first SeA (Figure 4, black arrows). Furthermore, the connection of the BA and DLAV on the irradiated side diminished (Figure 4, white arrowheads), and alternatively, the collateral blood vessel formed between the BA and PHBC (Figure 4, black arrowheads), whereas the BA in the nonirradiated side connected to the DLAV bending laterally (Figure 4, white arrows). We totally ablated 7 embryos (with the following condition: 70 mW, 8 ms) and observed the effects. The PHBC and DLAV of the ablated side were not connected in all the embryos (Figure 4, black arrows), whereas the bridge between the BA and DLAV (Figure 4, white arrowheads) diminished in 6 of the embryos. (In the rest, the ectopic vessel from the collateral vessel between the BA to PHBC connected to the DLAV.) To reconfirm the vascular formation of the ablated and nonablated first SeAs, we performed confocal microangiography. As a result, the disconnection between the BA, PHBC, and DLAV was clearly demonstrated on the ablated side (Figure V in the online-only Data Supplement). These ablation data for the first SeA are summarized in Figure 4C and 4D. To examine the influence of the overdose of irradiation to the surrounding tissues, we observed the targeted single endothelial cells by both bright-field and fluorescent microscopy before and after the irradiation (Figure VI in the online-only Data Supplement). After the ablation, the nuclear-localized fluorescence in the targeted cell weakened and finally diminished. Burn injury of the ablated cell was also confirmed in the bright-field image, whereas obvious defects to the cells in the surrounding tissues, such as the somites and neural tubes, could not be observed (we confirmed diminishment of the connecting vessels in this embryo). Furthermore, we stained some ablated embryos by 4',6-diamidino-2-phenylindole 16 to 18 hours after the ablation and observed it using confocal microscopy (Figure VII in the online-only Data Supplement). The obvious difference between the ablated and nonablated sides could not be confirmed. Taken together, the vessels diminished by the ablation of the first SeAs were well corresponded to the labeled vessel in Figure 3; therefore, these data are also useful to investigate the contribution of the first SeAs in the vascular morphogenesis between the brain and spinal cord.

Discussion

We applied the IR-LEGO system to the zebrafish vascular system to establish spatiotemporal gene regulation. Previous studies using electroporation,⁴ point laser,⁶ and the IR-LEGO system¹⁰ enabled only local gene regulation in vertebrates. In this study, we isolated each endothelial cell by using nucleus-localized enhanced green fluorescent protein and optimized the irradiation conditions needed to decrease gene induction in nontargeted cells. Thus, we achieved precise control of gene expression in single endothelial cells, which were extreme thin and contiguously surrounded by pericytes and muscle cells (Figure 2). Another single-cell gene expression system in zebrafish using a high-power pulse laser has recently been

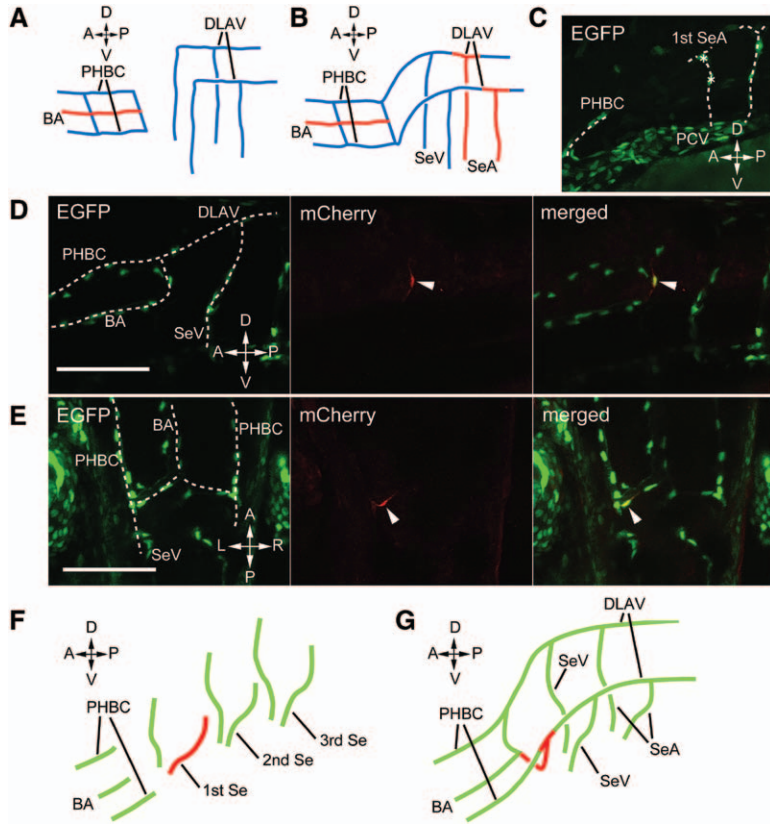


Figure 3. Integration of the vascular systems in the brain and spinal cord. **A** and **B**, Schematic illustrations of brain–spinal cord bridging at 1.5 dpf (**A**) and 2.0 dpf (**B**). This connection was formed in this period.¹¹ **C**, Endothelial cells of the first intersegmental artery (SeA; asterisks) and primordial hindbrain channel (PHBC) extending caudally in the *fli1:nEGFP* transgenic zebrafish embryo at 1.5 dpf before bridging. **D** and **E**, We labeled embryos at 1.5 dpf by using the infrared laser–evoked gene operator system through irradiation with three 1-s-long pulses from a 10.8-mW laser. The single endothelial cell of the first SeA labeled by laser-mediated gene induction of mCherry located in the bridging portion of basilar artery (BA) and dorsal longitudinal anastomotic vessel (DLAV; 18 hours after irradiation). Lateral view (**D**) and dorsal view (**E**). **F** and **G**, Schematic illustrations of labeling examination of first SeA at 1.5 dpf (**F**) and 2.0 dpf (**G**). The endothelial cells of the targeted first SeA are in red. **C–G**, Direction of the embryo is indicated for each figure. Scale bar, 100 μ m. A indicates anterior; D, dorsal; L, left; P, posterior; PCV, posterior cardinal vein; R, right; Se, intersegmental vessel; SeV, intersegmental vein; and V, ventral.

reported.¹² This system uses physical impulses of pulse irradiation for transferring injected material to the target cells from the surroundings, hence requires DNA or mRNA microinjection to the neighboring area for gene expression. This system does not require transgenic strains; hence, it is suitable for a nonmodel animal, but is not appropriate for our objectives. Recently, we revealed how the vasculature in the brain was developed during early ontogeny by time-lapse analysis (unpublished data). Gene regulation in the targeted single

endothelial cells *in vivo* will enable the analysis of the influence of a particular gene over the morphogenesis of each vessel in these regions.

Repeating the irradiation several times improved the efficiency of gene induction and led to a maximum induction rate of 60% (Table 2). However, the induction rate of nontargeted cells also rose by 3-fold. When the IR laser was used for irradiation, the endothelial cells shrunk as if evading the heat stress. The surrounding muscle cells may also contract after

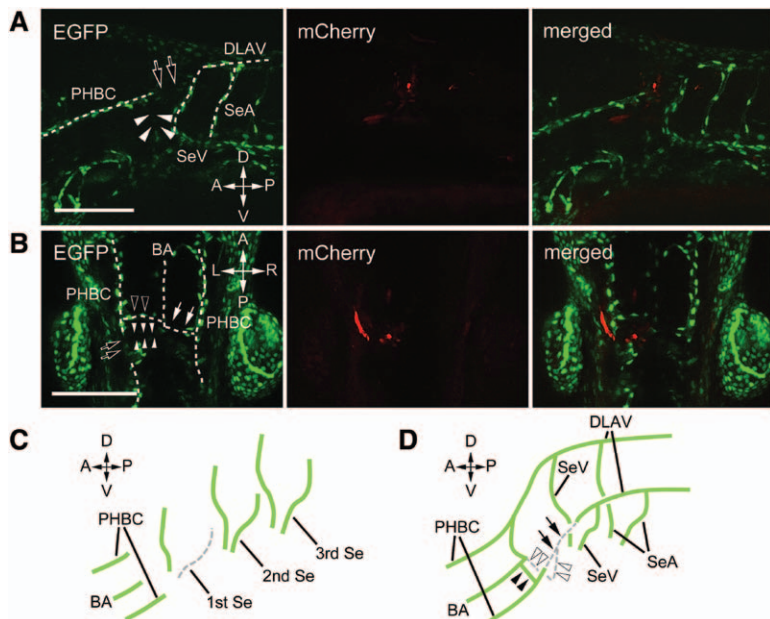


Figure 4. The connection of the vascular systems of the brain and spinal cord changed after the ablation of the first intersegmental artery (SeA). **A** and **B**, We ablated all endothelial cells of the unilateral first SeA using the infrared laser–evoked gene operator system, and observed them with CLSM 18 hours after the ablation. The gene expression of mCherry in the surrounding tissue was observed only on the ablated side. Lateral (**A**) and dorsal (**B**) views. On the ablated side, the bridging portions of the basilar artery (BA) and dorsal longitudinal anastomotic vessel (DLAV; **A** and **B** white arrowheads), and the primordial hindbrain channel (PHBC) and DLAV (**A** and **B** black arrows) diminished, and instead, the collateral vessel from the BA to PHBC formed (**B**, black arrowheads). **C** and **D**, Schematic illustrations of the ablation examination of the first SeA at 1.5 dpf (**C**) and 2.0 dpf (**D**). Normal vasculature that diminished on the ablated side is shown by a dotted gray line. **A–D**, The direction of the embryo is indicated in each figure. Scale bar, 100 μ m. A indicates anterior; D, dorsal; L, left; P, posterior; PCV, posterior cardinal vein; R, right; Se, intersegmental vessel; SeV, intersegmental vein; and V, ventral.

this stress and cause the irradiated endothelial cells to transfer. These movements seemed to influence the leakage of heat stress and made it difficult to diminish gene induction in non-targeted cells. Furthermore, applying the irradiating IR laser to the tissue resulted in intense heating of the elliptic region elongated vertically just before the focus,⁹ suggesting that the muscle cells located in the vertical region of the optical axis were easily influenced by the laser. We attempted some modification of the IR-LEGO system by interrupting the center of the irradiated laser before focusing and tried to reduce the leakage to the surrounding cells in the vertical region. Eliminating ectopic heating will require further improvements to the optical system in the IR-LEGO system. In contrast, we were able to achieve deletion of gene expression in the nontargeted cells from another viewpoint by using tissue-/cell-specific promoters and a recombination system. We then attempted to use the Cre-loxP system³ to reduce the minor leakage in nontargeted cells and establish double-transgenic zebrafish line with *hsp:Cre* and *kdrl:loxP:nlsGFP:loxP:mCherry* (the promoter of the *kdrl* gene also induces gene expression specifically in the endothelial cells). Using the embryos from these transgenic organisms, we noted that laser-mediated induction of the Cre gene only influenced the endothelial cells, in which the downstream effector of loxP sequence could be expressed by genome recombination of Cre. These improvements will elevate the value of IR-LEGO system as the precise in vivo gene regulation method in near future.

Because we succeeded in identifying the optimized condition of irradiation, we tried to label and trace the single endothelial cells of the first SeAs to elucidate their contribution to the connection between the vascular systems of the brain and spinal cord (Figure 3D and 3E). The tracing experiment with IR-LEGO system revealed that these endothelial cells bridged the BA to DLAV, and suggested that this system was valuable for fate-mapping analysis. We were able to trace strong mCherry expression in the targeted cells for >48 hours after induction. Lineage tracing analysis with time-lapse imaging of the *flt1:nEGFP* transgenic zebrafish was used to determine the source of the lymphatic endothelial cells to the thoracic duct.¹³ Although tracing backward in time the particular nucleus in time-lapse sequences was a useful method, the range of tracing the targeted cells was restricted to the imaging view. Transplantation of labeled cells or the labeling of individual cells by injecting heritable dye has been also used for tracing analysis and has provided useful products.¹⁴ However, these methods have been applied to the embryos only up to the mid-to-late blastula stages. In contrast, our method using the IR-LEGO system has no limitations for tracing the range and developmental stage, and therefore, it will be a powerful tool to map the fate of various cell types at later stages and to analyze the distribution or function of tissue-specific stem cells in various tissues, such as the digestive system.

Using the water heating property of the IR laser effectively, an overdose of laser irradiation was able to ablate the targeted cells. We ablated the endothelial cells of the first SeAs and assessed its influence on the connecting vessels between the brain and spinal cord. On the irradiated side, the connection between the BA and DLAV diminished, and the PHBC did not connect to the DLAV (Figure 4A and 4B). This suggested

the primary role of the first SeA in bridging BA and PHBC to DLAV, and the ablation experiment was a valuable method for analyzing the influence of the particular vessel on vascular morphogenesis.

By tracing and ablating the cells of the first SeAs, we clearly indicated their contribution to the connection between the vascular systems of the brain and spinal cord in zebrafish. In contrast, Padgett¹⁵ precisely described how these vascular systems were constructed by reconstructing serial sections of human embryos. In human embryos, the PHBC was identified at the 20-somite stage; the bilateral longitudinal neural arteries subsequently formed in the ventromedial region. Bilateral longitudinal neural arteries were medially fused to form the BA and were subsequently connected to the first SeAs. A zebrafish does not have a neck, and the final vascular systems in this region may greatly differ from those in human beings. However, the early processes, during which these vasculatures form, progress in a manner highly similar to that observed in humans; therefore, we believe that zebrafish can be considered a useful model to analyze the vascular formation between the brain and spinal cord. We are now very interested in the guidance mechanisms surrounding vascular formation in this region and are focusing on the perivascular tissues, such as the pericytes and mesenchymal cells, as well as the neural tissue. The IR-LEGO system will help us address this issue.

We demonstrated that the IR-LEGO system is a powerful tool with the potential to contribute to developmental biology. However, there are some limitations to this system. The most critical limitation is the depth of targeted cells. We achieved a maximum induction rate of 60% for the targeted single endothelial cells in the intersegmental vessels, which are usually located at a depth of 50 to 60 μm . The endothelial cells of the first SeA were localized at a depth of $\approx 70 \mu\text{m}$, which might cause a decrease in the efficiency of inducing gene expression in the tracing experiment. We assume that the limitation of gene induction in the single cells is at a depth of $\approx 100 \mu\text{m}$. The IR-LEGO system can be applied to various tissues at later developmental stages; however, the targeted region is restricted to a depth of 100 μm . We also indicated that the IR-LEGO system is useful for the ablation of single cells. Combining the ablation study with time-lapse imaging enables us to observe the regeneration process of ablated tissues. Induction of regeneration-associated genes after ablation will also contribute to understanding the underlying mechanisms.

In this study, we applied the IR-LEGO system to vascular biology and succeeded in demonstrating its usability in zebrafish. Our method enabled gene induction in single endothelial cells, tracing of targeted cells by fluorescent proteins, and ablation of the targeted vessel. Inducing the genes associated with vascular formation will help us to investigate the regulation of vascular connections. Furthermore, combined with small interfering RNA-mediated gene suppression, IR-LEGO will enable in vivo gene manipulation with vertebrate model organisms, and it leads to the prospect of uncovering the mechanisms underlying vascular morphogenesis.

Acknowledgments

We thank Dr Brant Weinstein (National Institutes of Health) for the transgenic zebrafish strain and Dr Ryozyo Nagai (Jichi Medical

University) for proofreading the article. We also thank Mutsumi Kurosawa, Taro Ando, Yohei Sawa, Yuki Matsumoto, and Motohiko Koizumi (Iwate Medical University) for the technical support offered for the screening and bleeding of the transgenic zebrafish, and we thank Misako Saida-Taniguchi (National Institute for Basic Biology) for offering technical support in optics.

Sources of Funding

This work was carried out under the National Institute for Basic Biology Cooperative Research Program (11-336) for E. Kimura and was supported by Grants-in-Aid for Scientific Research (KAKENHI) of Japan Society for the Promotion of Science (JSPS) grant number 23590222 (E. Kimura).

Disclosures

None.

References

1. Risau W. Mechanisms of angiogenesis. *Nature*. 1997;386:671–674.
2. Isogai S, Lawson ND, Torrealday S, Horiguchi M, Weinstein BM. Angiogenic network formation in the developing vertebrate trunk. *Development*. 2003;130:5281–5290.
3. Lakso M, Sauer B, Mosinger B Jr, Lee EJ, Manning RW, Yu SH, Mulder KL, Westphal H. Targeted oncogene activation by site-specific recombination in transgenic mice. *Proc Natl Acad Sci USA*. 1992;89:6232–6236.
4. Sato Y, Watanabe T, Saito D, Takahashi T, Yoshida S, Kohyama J, Ohata E, Okano H, Takahashi Y. Notch mediates the segmental specification of angioblasts in somites and their directed migration toward the dorsal aorta in avian embryos. *Dev Cell*. 2008;14:890–901.
5. Halloran MC, Sato-Maeda M, Warren JT, Su F, Lele Z, Krone PH, Kuwada JY, Shoji W. Laser-induced gene expression in specific cells of transgenic zebrafish. *Development*. 2000;127:1953–1960.
6. Ramos DM, Kamal F, Wimmer EA, Cartwright AN, Monteiro A. Temporal and spatial control of transgene expression using laser induction of the hsp70 promoter. *BMC Dev Biol*. 2006;6:55.
7. Feder ME, Hofmann GE. Heat-shock proteins, molecular chaperones, and the stress response: evolutionary and ecological physiology. *Annu Rev Physiol*. 1999;61:243–282.
8. Sato-Maeda M, Tawarayama H, Obinata M, Kuwada JY, Shoji W. Sema3a1 guides spinal motor axons in a cell- and stage-specific manner in zebrafish. *Development*. 2006;133:937–947.
9. Kamei Y, Suzuki M, Watanabe K, Fujimori K, Kawasaki T, Deguchi T, Yoneda Y, Todo T, Takagi S, Funatsu T, Yuba S. Infrared laser-mediated gene induction in targeted single cells in vivo. *Nat Methods*. 2009;6:79–81.
10. Deguchi T, Itoh M, Urawa H, et al. Infrared laser-mediated local gene induction in medaka, zebrafish and Arabidopsis thaliana. *Dev Growth Differ*. 2009;51:769–775.
11. Isogai S, Horiguchi M, Weinstein BM. The vascular anatomy of the developing zebrafish: an atlas of embryonic and early larval development. *Dev Biol*. 2001;230:278–301.
12. Hosokawa Y, Ochi H, Iino T, Hiraoka A, Tanaka M. Photoporation of biomolecules into single cells in living vertebrate embryos induced by a femtosecond laser amplifier. *PLoS One*. 2011;6:e27677.
13. Yaniv K, Isogai S, Castranova D, Dye L, Hitomi J, Weinstein BM. Live imaging of lymphatic development in the zebrafish. *Nat Med*. 2006;12:711–716.
14. Kimmel CB, Warga RM. Tissue-specific cell lineages originate in the gastrula of the zebrafish. *Science*. 1986;231:365–368.
15. Padgett DH. The development of the cranial arteries in the human embryo. *Contrib Embryol*. 1948;212:207–260.

Significance

In vivo spatiotemporal gene regulation in a single cell is obligatory to analyze specific gene functions associated with morphogenesis in developing embryos. The infrared laser-evoked gene operator system is a new microscopic method optimized to heat cells by using an IR laser, which has a superior ability to heat water and can efficiently access deep-lying tissues. We applied this method to the vascular system in zebrafish embryos and first succeeded in gene induction driven by heat shock promoter in the targeted endothelial cells. Inducing the particular genes using this method will help us to investigate the particular gene function in vivo. Additionally, combined with small interfering RNA-mediated gene suppression, infrared laser-evoked gene operator will enable in vivo gene manipulation in the future. Our achievement in this study will lead us to the prospect of uncovering the mechanisms underlying morphogenesis of vertebrate model organisms.

Supplement Material

Supplemental Figure I.

Construction of transgenic zebrafish lines and their fluorescent images at 3 dpf

(A) Each endothelial cell in the *fli1:nEGFP* transgenic zebrafish expresses nuclear-localized EGFP driven by the *fli1* promoter. (B) Cytoplasmic mCherry is induced by heat stress (38°C for 1 h) in the transgenic zebrafish with *hsp70:mCherry* several hours after stimulation. Scale bar = 1 mm.

Supplemental Figure II.

Time course of the laser-mediated gene induction

The mCherry expression was observed by fluorescent microscopy 2 (A), 4 (B), 6 (C), and 8 h (D) after irradiation, and by confocal microscopy 18 h after irradiation (E-G). The expression of mCherry in the targeted endothelial cells (C and D arrowheads) and non-targeted muscle cells (B-D arrows). DA: dorsal aorta; PCV: posterior cardinal vein. Scale bar = 200 µm.

Supplemental Figure III.

An example of laser-mediated gene induction with a 1-s-long single pulse of 12 mW IR laser (A) EGFP, (B) mCherry, and (C) merged image. Ten targeted single endothelial cells were irradiated, and mCherry expression in the targeted cells (arrowheads) was observed by confocal microscopy 18 h after irradiation. In this embryo, non-targeted cells did not express mCherry. Scale bar = 100 µm.

Supplemental Figure IV.

An example of laser-mediated gene induction with 3 pulses of IR laser at 10.8 mW for 1 s. (A) EGFP, (B) mCherry, and (C) merged image. Ten targeted single endothelial cells were irradiated, and mCherry expression in the targeted cells (arrowheads) and the non-targets (arrows) was observed by confocal microscopy 18 h after irradiation. Scale bar = 100 µm.

Supplemental Figure V

Microangiography of the vascular formation in the unilateral first SeA-ablated embryo

The unilateral first SeA-ablated embryo (70 mW for 8 ms) was microangiographed 18 h after ablation, and then laterally observed by confocal microscopy. Ablated side (A), and non-ablated side (B). On the ablated side, the connection between the BA, PHBC, and DLAV was diminished (white arrowheads). The direction of the embryo is indicated (A: anterior, P: posterior, D: dorsal, V: ventral). Scale bar = 100 µm.

Supplemental Figure VI

Ablation of the targeted endothelial cell by high-power flash irradiation

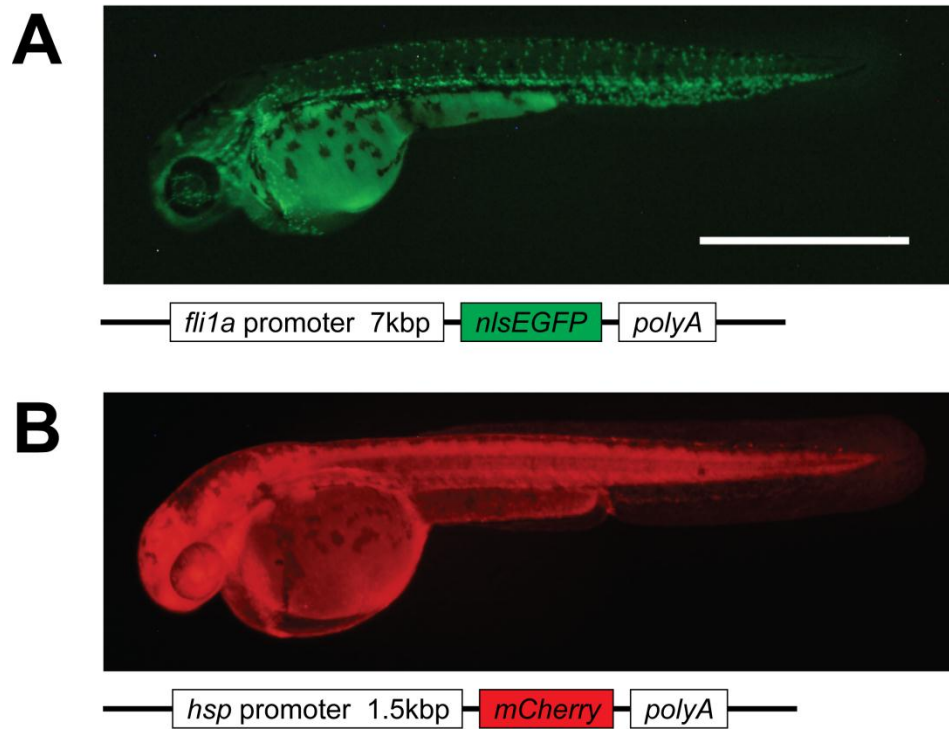
Bright-field (A, C) and fluorescent (B, D) images. Before (A, B) and after (C, D) irradiation of the targeted endothelial cells (arrowheads). After the ablation, burn injury to the ablated cells was confirmed (C), while obvious defects to cells in the surrounding tissues, such as the somites and neural tubes, could not be observed. The nucleus-localized fluorescence in the targeted cell weakened (D), and finally diminished (we confirmed the disconnection of the vessels in the embryo). The direction of the embryo is indicated (A: anterior, P: posterior, D: dorsal, V: ventral). Scale bar = 50 μ m.

Supplemental Figure VII

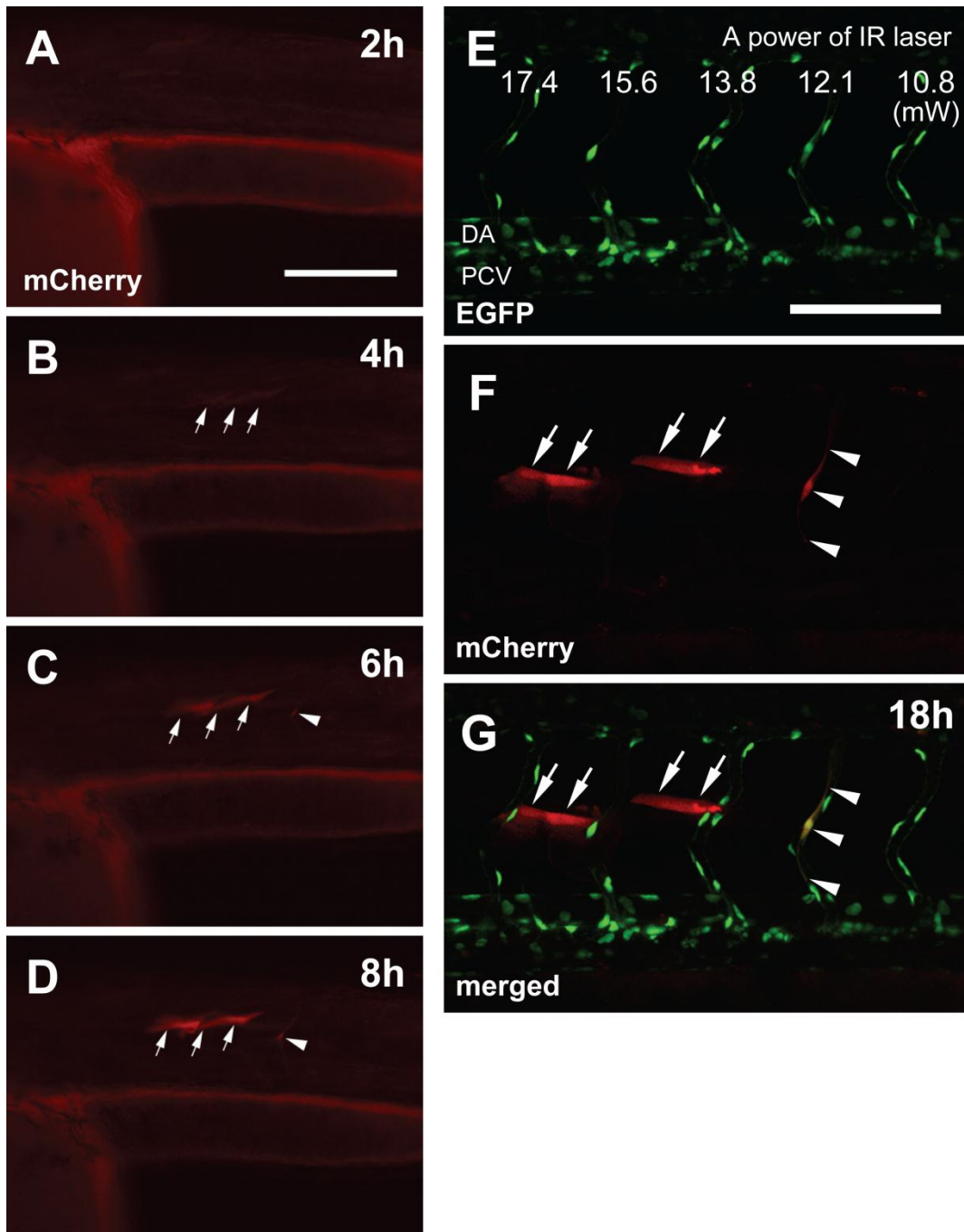
The influence of the ablation to the surrounding tissues

To examine whether the cells in the surrounding tissues of the irradiated first SeA, such as the somites or neural tubes, are damaged, we counter-stained some ablated embryos with DAPI 18 h after ablation. Merged images of EGFP and DAPI (A-E). Ventral (A) to dorsal (E) region. These images were observed as 10- μ m sliced images at 10- μ m intervals. Projected image of EGFP (F). Obvious damage could not be observed around the ablated region (white arrowheads). The direction of the embryo is indicated (A: anterior, P: posterior, R: right, L: left). Scale bar = 100 μ m.

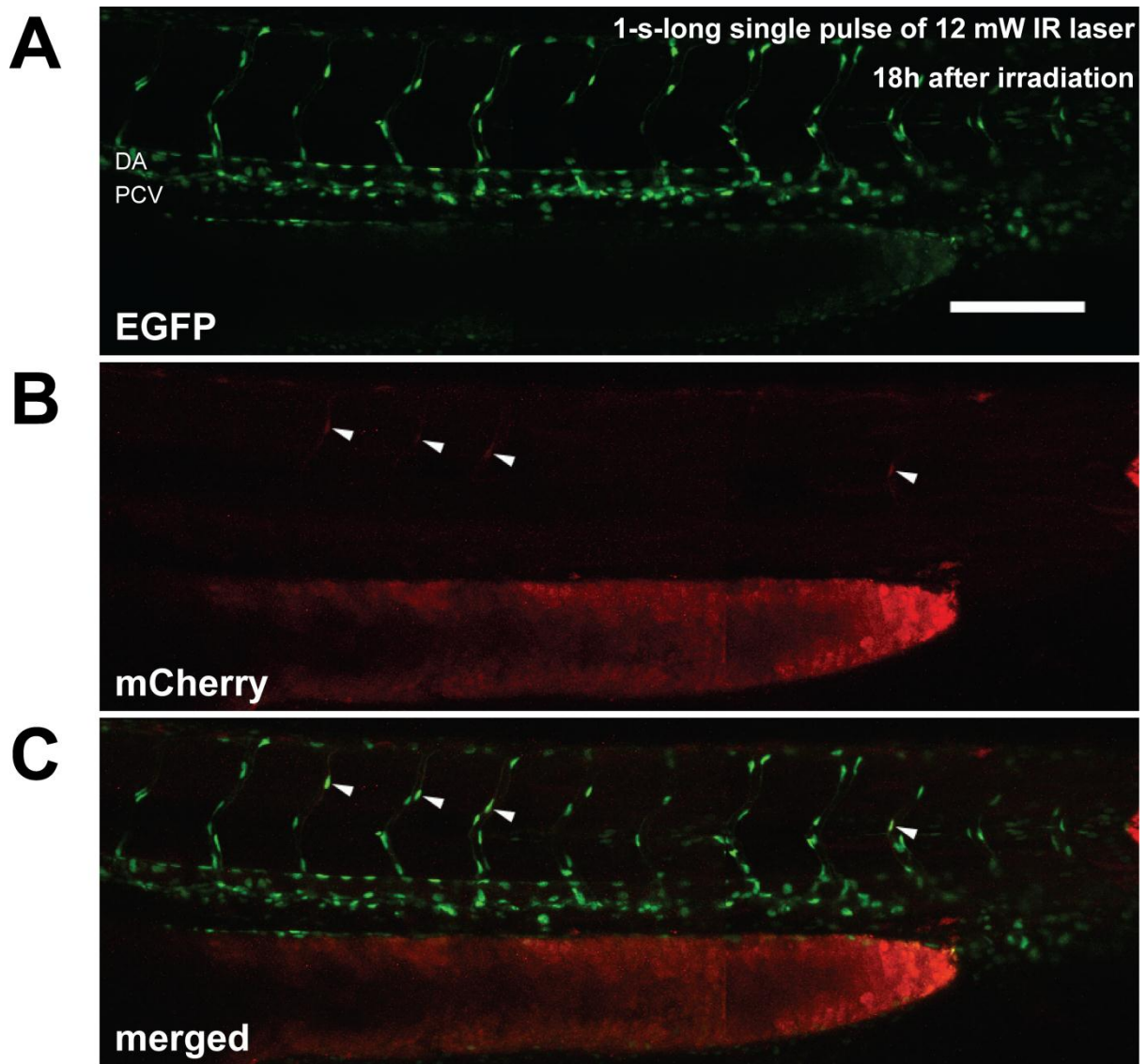
Supplemental Figure I.



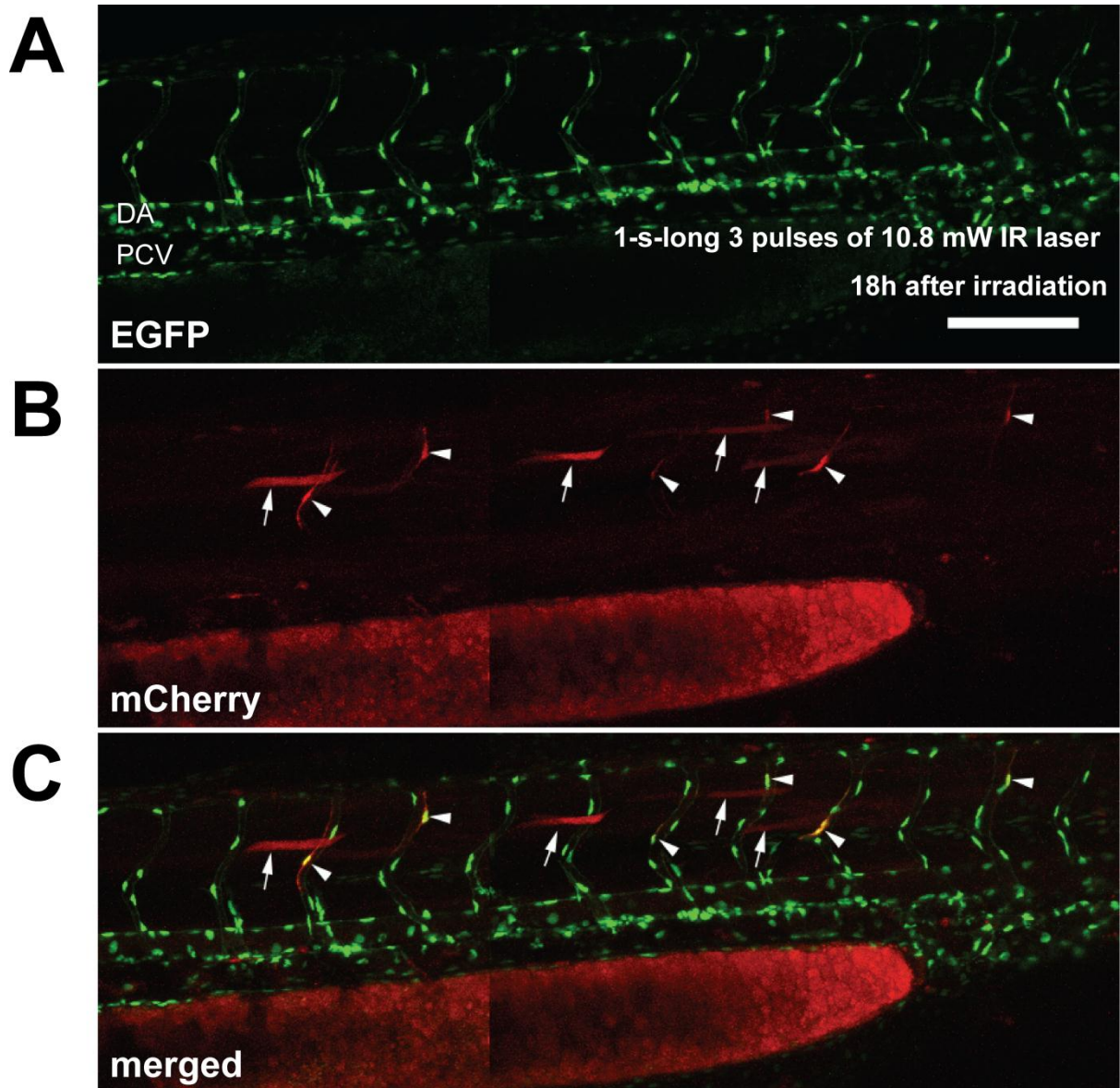
Supplemental Figure II.



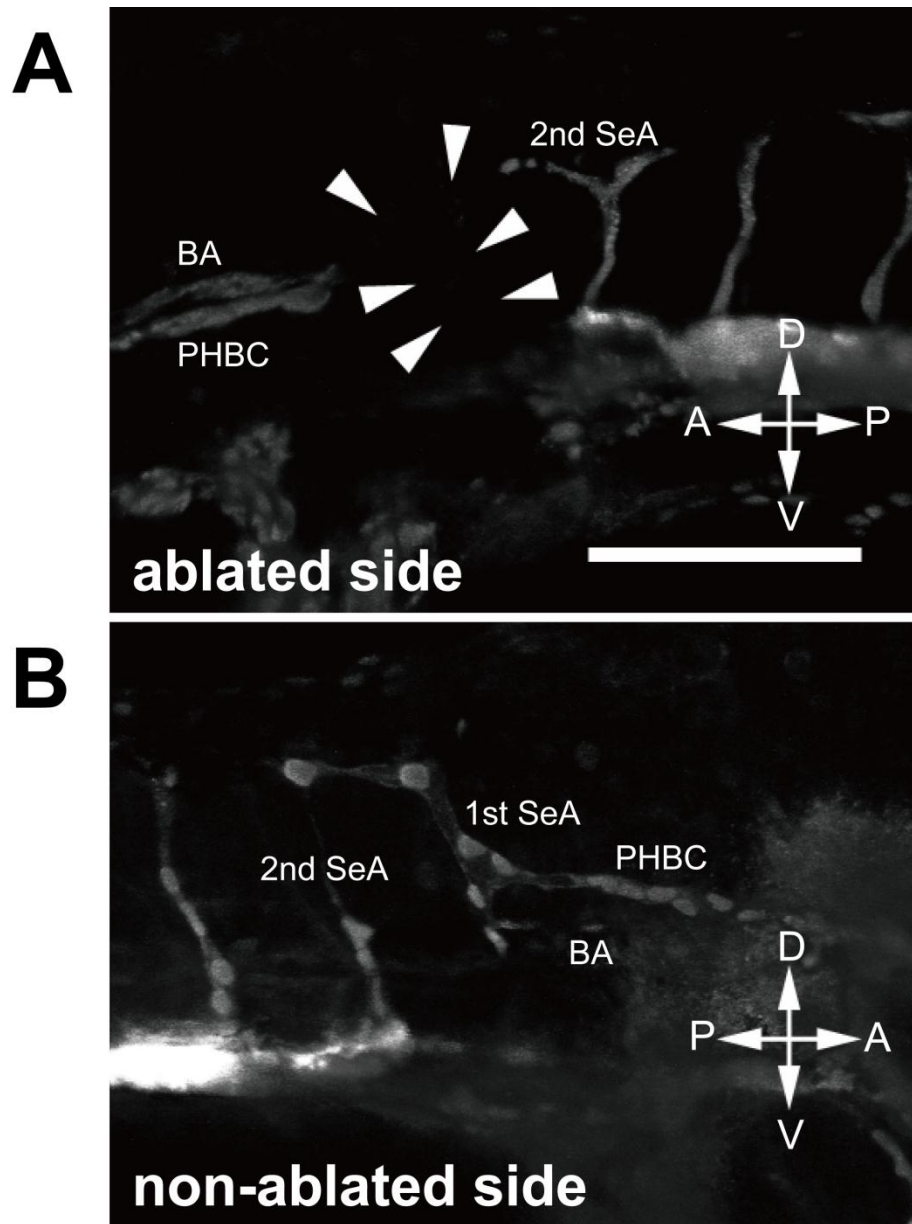
Supplemental Figure III.



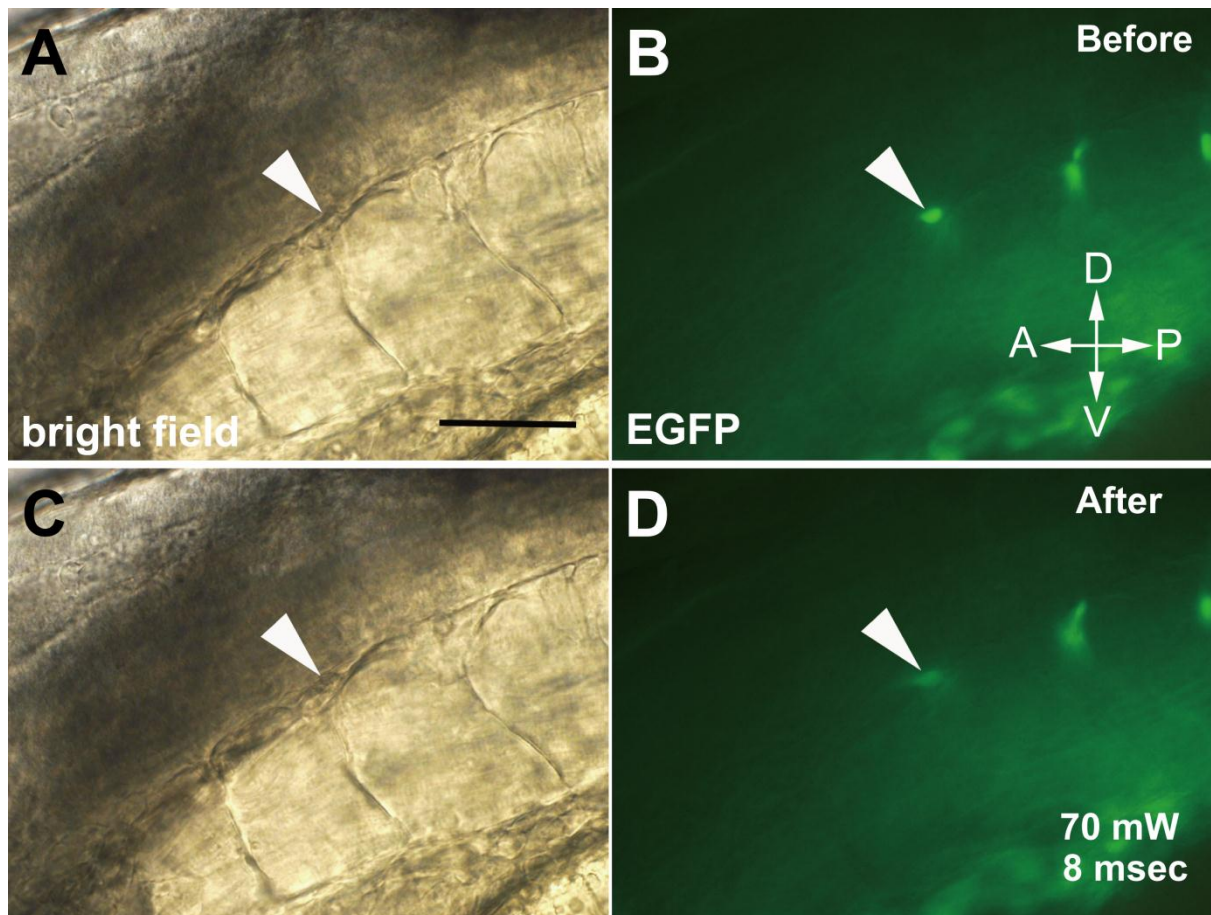
Supplemental Figure IV.



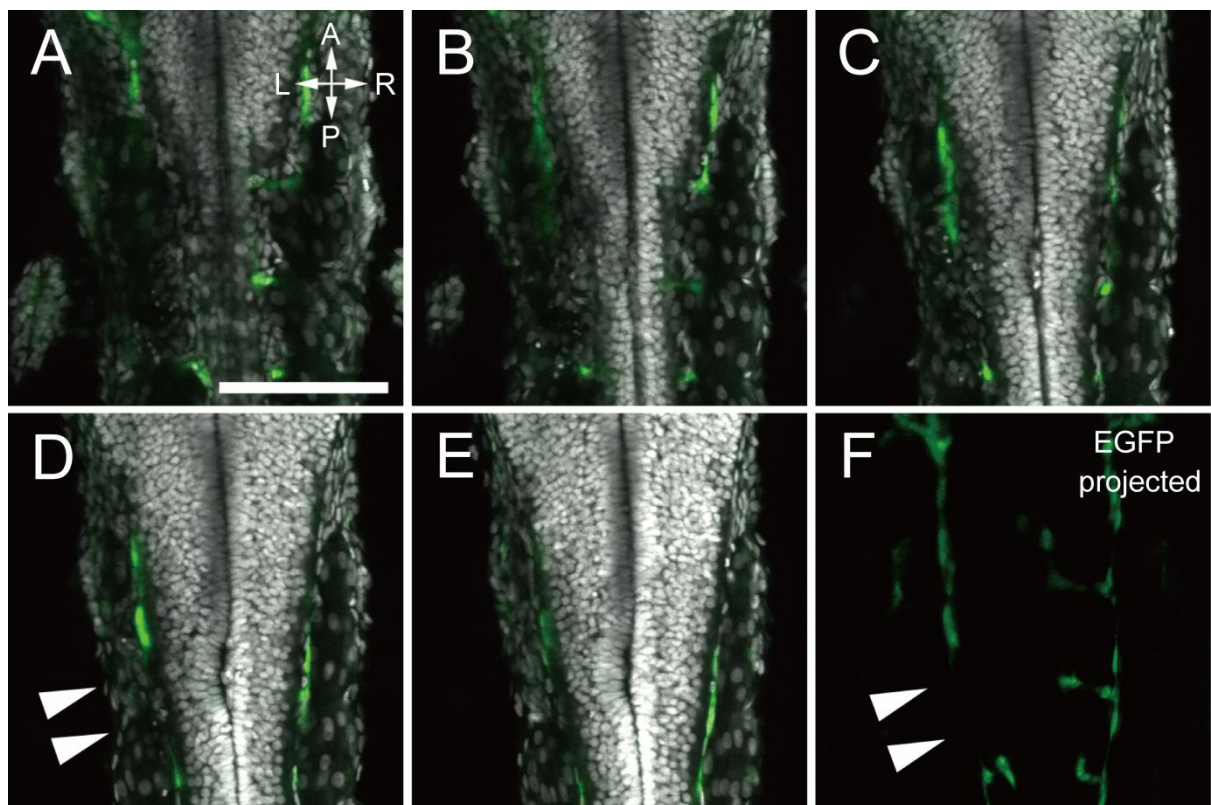
Supplemental Figure V.



Supplemental Figure VI.



Supplemental Figure VII.



Materials and Methods

Zebrafish (*Danio rerio*)

Zebrafish transgenic for *fli1:nEGFP* were provided from the Weinstein Lab (NIH), in which each endothelial cell was easily identified by nucleus-localized EGFP.¹ Zebrafish transgenic for *hsp:mCherry* were newly generated, in which heat stress induces the expression of cytoplasmic mCherry under the control of the zebrafish *hsp70* promoter. This promoter was almost always inactive during the embryonic stages without crystalline lens.^{2,3} The details of these lines are presented in Supplemental Figure I. We used double-transgenic zebrafish embryos that were obtained by mating the *fli1:nEGFP* and *hsp:mCherry* lines. The embryos were kept in conventional egg water at 23–25°C before and after irradiation, and staged by days post fertilization (dpf).⁴

IR-LEGO system and IR laser irradiation

The optical system of the IR-LEGO microscope has been described in detail in our previous reports.^{5,6} An IR-LEGO optical unit (IR-LEGO-1000; Sigma-Koki Co., Saitama, Japan) and a mono-coated objective lens (UApo340 20×/0.75 UV and UApo340 40×/0.9 UV; Olympus, Japan) were used for irradiation. The power of the IR laser was measured before irradiation by a power sensor on the IR laser (PD300-IR sensor; Ophir, Israel). Double-transgenic embryos (1.5–2 dpf) were first anesthetized with 0.02% Tricaine (M0387; Sigma) and embedded in cooled 0.5% low melt agarose to facilitate the stable positioning of the targeted endothelial cells. The experimental process of irradiation is summarized in Figure 1. We could judge whether the IR laser was precisely irradiating the targeted cells by transient reduction of fluorescent intensity, which originated with a property of fluorescent matter against temperature rise (Figure 1E, arrow). In contrast, a high-power flash irradiation of 70 mW IR-laser for 8-ms was used to ablate the single endothelial cells of first SeAs; ablation of the targeted cells was confirmed through the disappearance of their fluorescence immediately after irradiation.

Observation of laser-mediated gene expression

We first confirmed whether laser-mediated gene expression was induced in the targeted endothelial cells by using a fluorescent microscope (IX81; Olympus) 16–18 h after irradiation. Moreover, the mCherry fluorescence-positive embryos were observed with a confocal microscope (FV1000; Olympus or LSM5 Duo; Zeiss). To estimate the lag and duration time of the laser-mediated mCherry expression, we observed some embryos every 2 h after the irradiation by using the fluorescent microscope. The influence of the ablation of the first SeAs over the connecting portion of the vascular systems between the brain and spinal cord were also investigated by confocal microscopy with both lateral and dorsal views. To examine whether the cells in the surrounding tissues of the irradiated first SeA, such as the somites or

neural tubes, are damaged, we counter-stained some ablated embryos with DAPI and observed 10- μ m sliced images at 10- μ m intervals by confocal microscopy. Furthermore, we performed confocal microangiography to reconfirm the vascular formation of the embryos in which the first SeA was ablated.⁷

References

1. Roman BL, Pham VN, Lawson ND, Kulik M, Childs S, Lekven AC, Garrity DM, Moon RT, Fishman MC, Lechleider RJ, Weinstein BM. Disruption of *acvr1* increases endothelial cell number in zebrafish cranial vessels. *Development*. 2002;129:3009-3019.
2. Halloran MC, Sato-Maeda M, Warren JT, Su F, Lele Z, Krone PH, Kuwada JY, Shoji W. Laser-induced gene expression in specific cells of transgenic zebrafish. *Development*. 2000;127:1953-1960.
3. Nakayama S, Ikenaga T, Kawakami K, Ono F, Hatta K. Transgenic line with *gal4* insertion useful to study morphogenesis of craniofacial perichondrium, vascular endothelium-associated cells, floor plate, and dorsal midline radial glia during zebrafish development. *Dev Growth Differ*. 2012;54:202-215.
4. Kimmel CB, Ballard WW, Kimmel SR, Ullmann B, Schilling TF. Stages of embryonic development of the zebrafish. *Dev Dyn*. 1995;203:253-310.
5. Kamei Y, Suzuki M, Watanabe K, Fujimori K, Kawasaki T, Deguchi T, Yoneda Y, Todo T, Takagi S, Funatsu T, Yuba S. Infrared laser-mediated gene induction in targeted single cells *in vivo*. *Nat Methods*. 2009;6:79-81.
6. Deguchi T, Itoh M, Urawa H, et al. Infrared laser-mediated local gene induction in medaka, zebrafish and *Arabidopsis thaliana*. *Dev Growth Differ*. 2009;51:769-775.
7. Isogai S, Horiguchi M, Weinstein BM. The vascular anatomy of the developing zebrafish: an atlas of embryonic and early larval development. *Dev Biol*. 2001;230:278-301.